

LIQUEFACTION ANALYSIS OF VERIFICATION ON THE INFLUENCE OF UNDERGROUND STRUCTURE

*Keita Sugito¹, Tetsuya Okano² and Ryoichi Fukagawa³

^{1,2}Graduate School of Science and Engineering, Ritsumeikan University, Japan; ³Department of Science and Engineering, Ritsumeikan University, Japan

*Corresponding Author, Received: 25 Oct. 2018, Revised: 29 Dec. 2018, Accepted: 14 Jan. 2019

ABSTRACT: It is widely recognized that the Kansai area will be attacked by a plate boundary type huge earthquake within these 30 years. When the earthquake happens, the ground with underground structure, like a tunnel, would be struck by severe liquefaction disasters. Therefore, we tried to analyze the ground behavior using LIQCA, which is well used for liquefaction analysis in Japan. The input earthquake motion is the seismic standard spectrum I which is commonly used in Japan. The ground has the underground structure, so we investigated not only the liquefaction phenomenon of the ground itself but also the behavior of the underground structure. Furthermore, we focused on the boundary condition between the tunnel and the adjacent ground. Three patterns are prepared for this boundary condition. First, the boundary condition between the tunnel and the ground is free in the vertical direction and fixed in the horizontal direction. Second, this boundary condition is fixed in the vertical direction and the horizontal direction is fixed. Third, the joint elements are installed between the tunnel and the ground. Under each condition, we examine the effect of liquefaction on the tunnel. Also, we compare the three patterns and verified realistic damage.

Keywords: Liquefaction, Numerical simulation, Tunnel, Float up

1. INTRODUCTION

There is a high probability of a large, plate boundary-type earthquake occurring within 30 years in the Kansai area, Japan. The western part of the country will be severely damaged by this earthquake. In particular, the Osaka Gulf coast is predicted to suffer from a severe liquefaction disaster [1]. Therefore, a liquefaction simulation was applied to a typical site on the Osaka Gulf coast. The simulation is based on the LIQCA [2] program, which is widely used as a liquefaction simulation tool in Japan. The target ground has an underground tunnel; it is known that liquefaction affects tunnels, but concrete indications of it have not been found. So, we investigated not only the liquefaction phenomenon of the ground itself but also the behavior of the underground structure. During the simulation, by changing the boundary condition between the tunnel and the adjacent ground, the difference in the amount of the tunnel floating when liquefaction occurs should be noted.

2. OUTLINE OF ANALYSIS

2.1 Ground to Be Analyzed

The analysis target is some area on the Osaka Gulf coast, which is characterized by alluvium deposits. Fig.1 shows the cross section of this target; the cross section has a length of 100 m in the

horizontal direction and a depth of 40 m. The tunnel is located near the surface in the center of the ground. The soil layers that may liquefy are the As1, As2 and Tsg1 layers. Other layers are composed of clayey soil and hard sandy soil, and thus, their liquefaction is not considered to be a significant risk.

The groundwater level is set at GL-2.3 m. The Oc layer is the basal surface in this cross-section. The B layer, the layer above the groundwater level, is considered hard to liquefy, so the Ramberg-Osgood model is applied to this layer. The layer below the groundwater level is modeled by the cyclic elastoplastic constitutive model. Table 1 lists the material parameters used in the analysis. The liquefaction layers and non-liquefaction layers are fitted based on the respective standards. The liquefaction layers have liquefaction strength curves based on the Design Standards for Railway Structures and Commentary [3]. The shear modulus and shear strain relationship ($G/G_{\max} \sim \gamma$), historical attenuation and shear strain relationship ($h \sim \gamma$) were referenced using element simulations. These were used to determine the nonlinear properties of the non-liquefaction layers. Since $G/G_{\max} \sim \gamma$ and $h \sim \gamma$ relationship are different for each soil, and these relationships are highly dependent on the constraining pressure, it is preferable to calculate these variables by an indoor test, such as a repeated triaxial test of the sampled specimen. The non-liquefaction layers are fitted to the Yasuda-Yamaguchi model [4].

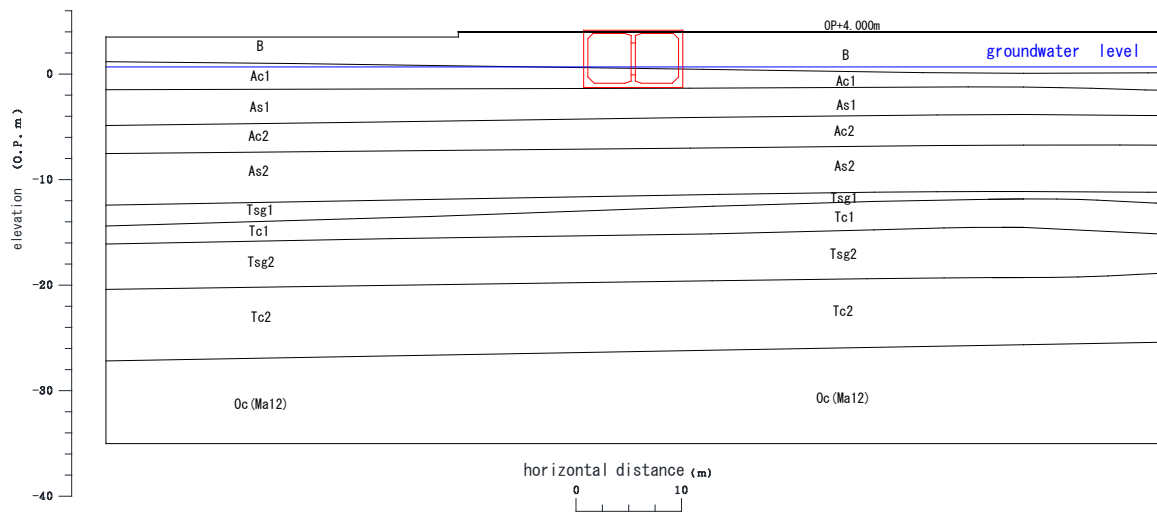


Fig.1 Cross section of the target area

Table 1 List of material parameters

	①	②	③	④	⑤	⑥	⑦	⑧	⑨	
	B	As1	Ac1, Ac2	As2	Tsg1	Tc1	Tsg2	Tc2	Oc	
type	Y	X	X	Y	X	Y	Y	Y	Y	
γ (kN/m ³)	18.0	18.0	18.0	16.0	18.0	16.0	18.0	16.0	16.0	18.0
ρ (g/cm ³)	1.8	1.8	1.8	1.6	1.8	1.6	1.8	1.6	1.6	1.8
k (m/s)	1.47	1.47	1.47	9.00	5.17	2.60	1.20	1.00	7.50	1.12
e_0	E-06	E-06	E-06	E-09	E-06	E-07	E-05	E-07	E-09	E-06
V_s (m/s)	0.658	0.658	0.990	1.038	0.505	0.724	0.777	1.098	1.799	0.673
λ	120	140	120	120	240	200	260	208	208	170
κ		0.002	0.002		0.001					0.1
OCR*		0.025	0.02		0.001					0.02
G_0/σ'_{m0}		1.3	1.0		1.6					1
M_m^*		935.5	445.3		1104					646.1
M_f^*		0.909	0.909		0.909					0.909
B_0^*		1.012	0.966		1.215					0.958
B_1^*		3500	2500		10000					5000
C_f		80	50		20					100
γ_r^{p*}		0	0		0					0
γ_r^{E*}		0.02	0.002		0.005					0.02
D_0^*		0.001	0.3		0.001					0.3
n		1.0	1.5		4.0					4
C_d		7.0	2.0		8.0					6
v		2000	2000		2000					2000
c (kPa)	0.496			0.496		0.494	0.488	0.492	0.492	
φ (deg)	0			33		198	0	149	149	
a	30.9			0		0	34	0	0	
b	6977			2241		4939	8530	4533	4165	
α	0.5			0.5		0.5	0.5	0.5	0.5	
r	1.89			16.7		2.3	2	1.4	1.5	
	1.92			1.78		2.1	3	1.7	1.6	

Notations: X: cyclic elastoplastic constitutive model, Y: R-O model, γ : unit weight, ρ : density, k : coefficient of permeability, e_0 : initial void ratio, V_s : shear wave velocity, λ : compression index, κ : expansion index, M_f : stress ratio parameter corresponding to failure angle, OCR^* : factoid overconsolidation ratio, G_0/σ'_{m0} : non-dimensional initial shear modulus, M_m : stress ratio parameter corresponding to phase transformation angle, B^*_0 , B^*_1 , and C_f : plastic modulus parameters, γ_r^{P*} : plastic strain, and γ_r^{E*} : elastic strain, D^*_0 , n : dilatancy coefficient, C_d : anisotropy elimination parameter, ν : Poisson's ratio, c : cohesion, ϕ : internal friction angle, and a , b , α , and r : R-O parameters

2.2 Tunnel Model

Fig.2 shows a model of the tunnel within the ground. The yellow lines indicate the structure of the tunnel. The tunnel consists of an upper and lower base plate, a sidewall, and a center pillar. The structure of this tunnel is represented by a beam element. Table 2 lists the tunnel parameters used in the analysis. B is the horizontal length of the element, and H is the vertical length of the element. The tunnel is comprised of four kinds of boards.

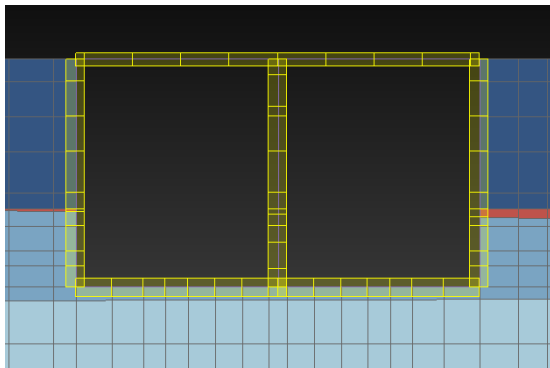


Fig.2 Tunnel model

Table 2 Tunnel parameters

	upper	lower	side	center
B (m)	1	1	1	2.3
H (m)	0.3	0.4	0.4	0.4
Pitch (m)	1	1	1	4
γ (kN/m ³)	25	25	25	25
A (m ²)	0.3	0.4	0.4	0.92
I (E-03m ⁴)	1.13	2.67	2.67	6.00
G (kN/m)	7.5	10	10	5.75

Notations: γ : Unit volume weight, A : Sectional area, I : Sectional Secondary moment, G : Unit length Weight

2.3 Boundary Conditions

2.3.1 Soil Skeleton

In the analysis model, the bottom of the boundary is an elastic base (viscous boundary). The elastic base is placed as a dashpot on the bottom of the model. The input earthquake motion is a 2E wave. In LIQCA, only the horizontal lower boundary can be set for the viscous boundary. When a consolidation analysis is conducted, the dashpot is automatically replaced with a rigid spring. The side boundary is a method of connecting a wide free ground part, which is not easily influenced by the FEM region, to the side surface when the soil layer configuration of the side boundary is different.

2.3.2 Tunnel

Three patterns are prepared for this boundary condition. First, the boundary condition between the tunnel and the ground is free in the vertical direction and fixed in the horizontal direction; the boundary condition between the tunnel and adjacent ground is free from friction in the vertical direction, and the tunnel and its adjacent ground behave similarly in the horizontal direction. The second boundary condition is fixed in both the vertical and horizontal directions. The friction between the tunnel and the ground is set not to be lost in both the horizontal direction and the vertical direction. In the third pattern, joint elements are installed between the tunnel and the ground. A joint element is a model that can install a virtual spring, which takes sliding and peeling between the structure and the ground into account. Parameters are set as shear direction spring constant $k_s = 5.0 \times 10^5$ (kN/m²) and vertical direction spring constant $i_n = 5.0 \times 10^5$ (kN/m²). We refer to a method of making these magnitudes about 10 times larger than the spring constant of the adjacent ground [5].

2.4 Input earthquake motion

The input earthquake motion is the seismic standard spectrum I, which is commonly used in Japan. The waveform is shown in Figure. 3. The increment of the calculation time is 0.005 s. The Newmark method coefficients are $\beta = 0.3025$ and $\gamma = 0.6$. These values are common in LIQCA simulations. The constant of the Rayleigh attenuation (α_1) is equal to 0.001–0.003. After the seismic motion, consolidation analysis is carried out until the vertical settlement converges.

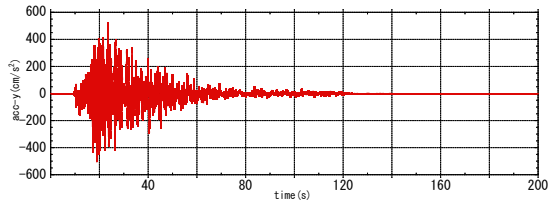


Fig.3 Waveform of the seismic standard spectrum I

2.5 Initial stress analysis

The initial values of the soil skeleton displacement and excess pore water pressure are all 0. The soil skeleton displacement and excess pore water pressure in LIQCA are the increments from the initial state, that is, the incremental values at the time of the earthquake. Under these initial conditions, it is necessary to set the initial effective stress of the ground. Therefore, it is important to estimate the initial stress state in the ground, which was completed by a self-weight analysis. The self-weight analysis calculates the initial stress by applying self-weight to the model used for the liquefaction analysis in the zero-gravity state. It considers the increase in ground rigidity and nonlinearity caused by adding weight to the model.

3. ANALYSIS RESULT

The analysis results are shown below. After the earthquake motion, a consolidation analysis was carried out until the convergence of the vertical displacement was confirmed. The effective stress decreasing ratio (ESDR) is used as an index for determining liquefaction. It is shown in the following equation:

$$ESDR = 1 - \frac{\sigma_m}{\sigma_{m0}} \quad (1)$$

σ_m : average effective stress corresponding to some elapsed time (kN/m²)

σ_{m0} : average effective stress in the initial stress state (kN/m²)

When this value reaches 1, liquefaction occurs in the ground. The results can be divided into three patterns according to the boundary condition between the tunnel and the adjacent ground, as previously mentioned. The analysis results are summarized according to these three patterns.

3.1 Free Boundary Condition

Fig.4 shows the ESDR values of the ground layers As1, As2, and Tsg1. These results indicate that these soil layers become liquefied during a large earthquake. The effective stress reduction ratio decreases after 10⁸ s (approximately 3 years).

This indicates that the excess pore water pressure that occurs by liquefaction is dissipated and that the consolidation settlement converges. Fig.5 shows the vertical displacement of the tunnel during the earthquake. After the consolidation of the soil, the tunnel has risen by 0.9 m.

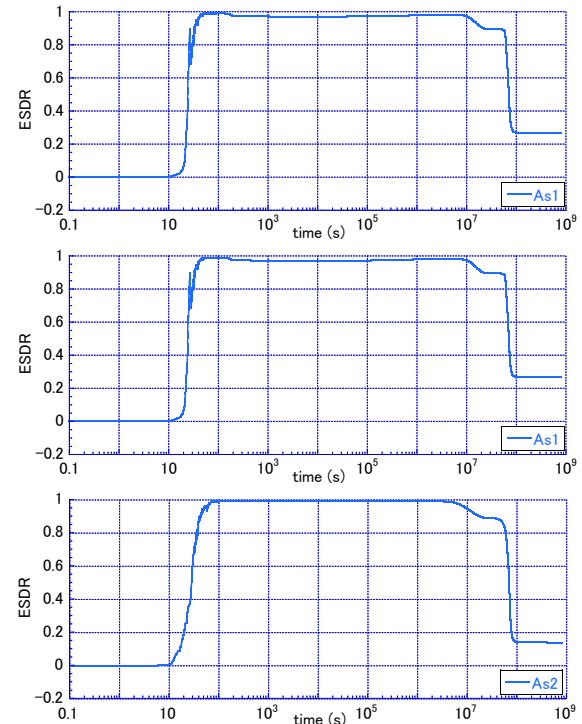


Fig.4 Effective stress decreasing ratio of As1, As2, and Tsg1

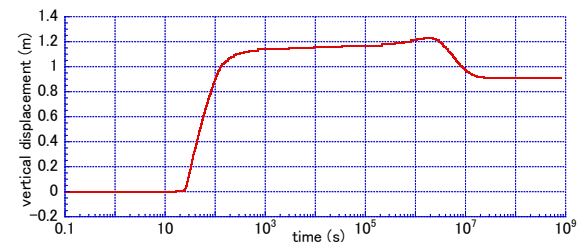


Fig.5 Vertical displacement of the tunnel under the free boundary conditions

3.2 Fixed Boundary Condition

Fig.6 shows the ESDR value of As1, As2, and Tsg1 under the fixed boundary condition. Under these conditions, the results indicate that these layers do become liquefied. This indicates that the excess pore water pressure that occurs by liquefaction is dissipated and that the layers consolidate. Fig.7 shows the vertical displacement. After the consolidation of the layers, the tunnel settles by 0.2 m.

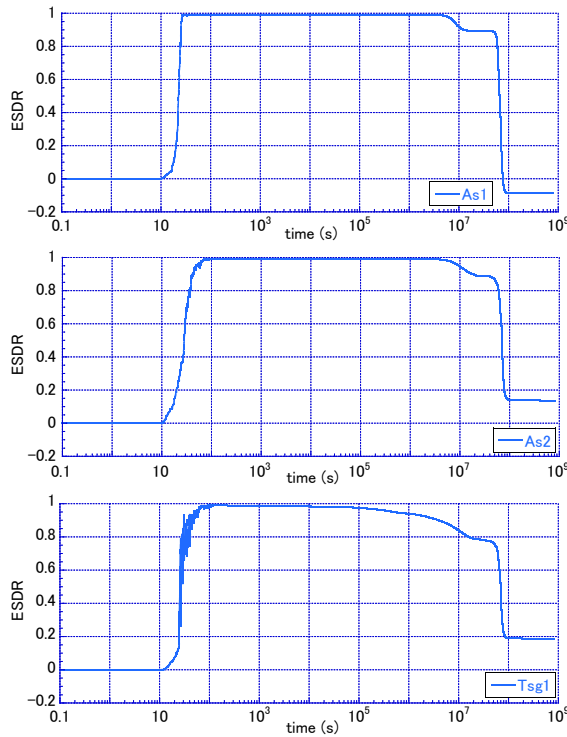


Fig.6 Effective stress decreasing ratio of As1, As2, and Tsg1

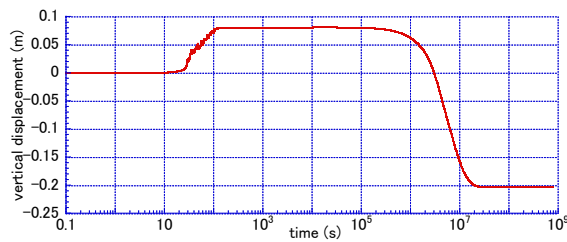


Fig 7 Vertical displacement of the tunnel under the fixed boundary conditions

3.3 Joint Element

Fig.8 shows the ESDR of the soil layers As1, As2, and Tsg1 under the addition of the joint element. As with the previous models, the results show that the layers do become liquified under strong ground motion. This indicates that the excess pore water pressure dissipates, and the soil layers undergo consolidation. Fig.9 shows vertical displacement, after consolidation, the tunnel rises by 0.8 m. It is considered that the parameter of the joint element affects the uplifting of the tunnel seen at liquefaction occurrence.

3.4 Displacement of the Ground Surface

Fig.10 shows the vertical displacement for each time history. The data corresponds to the state of the

initial coordinate and vertical coordinate of three patterns after the consolidation of the ground surface coordinates.

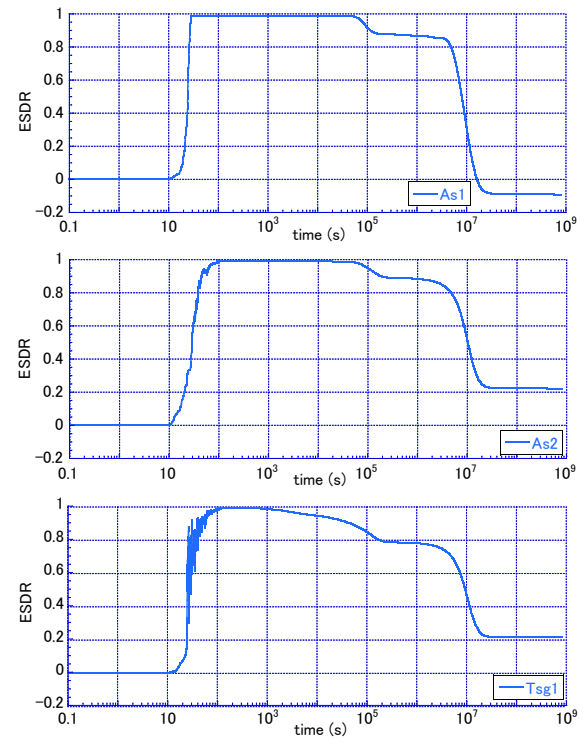


Fig.8 Effective stress decreasing ratio of As1, As2, and Tsg1

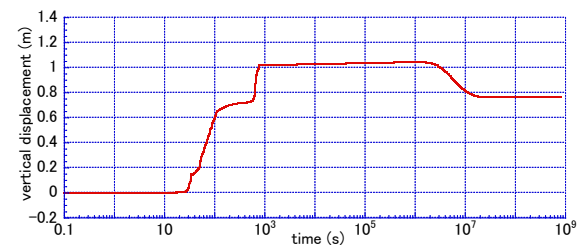


Fig.9 Vertical displacement of the tunnel in the joint element condition

The tunnel is located between 45 and 55 m along the X-axis. In the rest of the cross-section, both the free and joint element models show almost the same amount of settlement. The tunnel was uplifted most under the free boundary conditions but settled under fixed boundaries. The phenomenon observed under the free boundary condition is caused by the lack of vertical friction between the side surface of the tunnel and the surrounding ground. Therefore, a rise of 0.9 m is thought to be the maximum floating amount. The fixed boundary condition is not thought to be realistic because it is supposed that the friction between the tunnel and the adjacent ground is not lost when liquefaction occurs. The joint element model takes into consideration the reduction in shear strength due to the rise of excess

pore water pressure, which is observed when liquefaction occurs. Even assuming actual phenomena, peeling and slipping may occur at the boundary between the tunnel and the ground, and so the use of joint elements is appropriate.

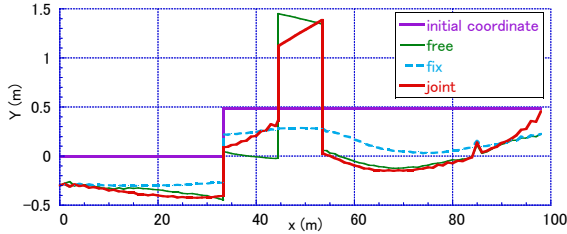


Fig.10 Vertical displacement for each time history

4. CONCLUSION

When an earthquake, corresponding to seismic standard spectrum I, occurs at the target ground of the Osaka Gulf coast, the results of a liquefaction simulation based on LIQCA indicate that the ground becomes liquefied and the tunnel at the surface of the target ground rises by between 0.8 m and 0.9 m. This phenomenon is caused by the boundary condition between the tunnel and the surrounding ground. Although the boundary between the tunnel and the adjacent ground can be modeled to some extent using the joint elements model, it is still necessary to make this phenomenon

more realistic. The buoyancy problem may be difficult to reconcile, and therefore, this paper will further investigate the boundary condition between the sidewall of the tunnel and the adjacent ground to conduct more realistic simulations.

REFERENCES

- [1] Matsuoka S, Wakamatsu K, and Hashimoto K., "Estimation method of liquefaction risk based on topography: Ground classification 250 m mesh map", in Proc. of the Japan Earthquake Engineering Association, 2011, pp. 35–36.
- [2] LIQCA Liquefaction Geo-Research Institute., LIQCA 2 D 15 · LIQCA 3 D 15 material, 2015.
- [3] Railway Technical Research Institute., Design Standards for Railway Structures and Commentary, 2012.
- [4] Yasuda S, and Yamaguchi I., "Dynamic deformation characteristics of various undisturbed soils", of the 20th Soil Engineering Research Presentation, 1985, pp. 539–542
- [5] Civil Engineering Association Partial, Dynamic Analysis Method, Dynamic Analysis and Seismic Design Vol. 2, Gihodo Shuppan Publishing, 1989, pp.123– 125

Copyright © Int. J. of GEOMATE. All rights reserved, including the making of copies unless permission is obtained from the copyright proprietors.
